Chemistry & Biology, Vol. 11, 807–815, June, 2004, ©2004 Elsevier Ltd. All rights reserved. DOI 10.1016/j.chembiol.2004.03.029

High-Throughput Ribozyme-Based Assays for Detection of Viral Nucleic Acids

Karl Kossen,[1] Narendra K. Vaish,[1,3] Vasant R. Jadhav,[1,3] Christopher Pasko,[1,5] Hong Wang,[2] Robert Jenison,[2] James A. McSwiggen,[1] Barry Polisky,[1,*] and Scott D. Seiwert[1,4,*]
[1]Sirna Therapeutics, Inc.
2950 Wilderness Place
Boulder, Colorado 80301
[2]Thermo Electron, Corp.
Point of Care and Rapid Diagnostics
331 S. 104th St.
Louisville, Colorado 80027

Summary

Many reports have suggested that target-activated ribozymes hold potential value as detection reagents. We show that a "half"-ribozyme ligase is activated similarly by three unstructured oligoribonucleotides representing the major sequence variants of a hepatitis C virus 5′-untranslated region (5′-UTR) target and by a structured RNA corresponding to the entire 5′-UTR. Half-ribozyme ligation product was detected both in an ELISA-like assay and in an optical immunoassay through the use of hapten-carrying substrate RNAs. Both assay formats afford a limit of detection of approximately 1×10^6 HCV molecules (1.6 attomol, 330 fM), a sensitivity which compares favorably to that provided by standard immunoassays. These data suggest that target-activated ribozyme systems are a viable approach for the sensitive detection of viral nucleic acids using high-throughput platforms.

Introduction

Applications ranging from basic research to molecular diagnostics require the sensitive detection of nucleic acids. We recently described a new class of target-activated ribozymes, which we termed "half"-ribozymes [1], that are based on 3′-truncated class I ligases [2–5]. Half-ribozymes are active only when bound to a specific *trans*-acting nucleic acid that supplies the deleted sequence, allowing the ligation of two substrate RNAs to be used as a readout for the presence of a target nucleic acid. The catalytic nature of half-ribozymes allows for a single molecular recognition event to facilitate multiple RNA-ligation reactions and therefore provides a signal amplification step for target detection. Iterative RNA selection techniques can be used to develop half-ribozymes activated by different target sequences, suggesting that this approach for nucleic acid detection is generally applicable [1].

Half-ribozymes are considerably more sensitive than other ribozyme-based approaches for nucleic acid detection. The half-ribozyme previously developed that is activated by a sequence in the 5′-UTR of hepatitis C virus (HCV) is capable of detecting zeptomole quantities (~7000 copies) of its target nucleic acid, a sensitivity of detection roughly 1×10^6-fold greater than that observed in other ribozyme-based systems [1, 6]. The greater sensitivity is attributed to the absence of target-independent ribozyme catalysis, which is a facet of other ribozyme-based detection systems [6–12]. The increased rate differential between target-activated catalysis and background ligation (~2.6×10^9-fold; [1]) relative to other ribozyme-based detection systems (1×10^4-fold; [6]) translates directly into the increased sensitivity provided by half-ribozymes. Indeed, this rate differential was used to predict the sensitivity of detection that was demonstrated in an assay employing detection of radiolabeled product RNA [1].

In the present work, we investigated whether this HCV-activated half-ribozyme is capable of detecting natural sequence variants of its target, whether functional target can be readily derived from a large, structured RNA, and whether half-ribozymes are compatible with immunodiagnostic detection platforms.

Results and Discussion

The half-ribozyme previously developed is activated by a conserved sequence in the 5′-untranslated region (5′-UTR) of the hepatitis C virus [1]. Although this target represents one of the most highly conserved portions of the HCV genome, it is not universally conserved in reported HCV sequences. Therefore, we investigated whether naturally occurring variants of the HCV target could activate half-ribozyme catalysis in order to establish whether the HCV sequence-activated half-ribozyme could act as a general HCV-detection reagent.

Since 1431 sequences corresponding to the 5′-UTR of HCV are deposited in GenBank, the variation of this sequence can be robustly investigated. Remarkably, only three different target sequences represent ~80% of all GenBank entries of the 5′-UTR [1]. The most prevalent sequence, which is found in 66.3% of GenBank entries, was used to initially generate the HCV-activated half-ribozyme (target 1 in green, Figure 1A). The second most prevalent sequence, which represents 8.3% of GenBank entries, changes an A-U base pair at position 15 to a noncanonical G-U base pair, replaces a C-G base pair at position 19 with an A/G internal bulge, and replaces an internal C/A bulge at position 23 with an U-A base pair (target 2, Figure 1A). The next most prevalent sequence (5.1% of GenBank entries) carries a single base change that replaces a C-G base pair at position 19 in the target-half-ribozyme duplex with a noncanonical U-G base pair (target 3, Figure 1A).

*Correspondence: sseiwert@intermune.com (S.D.S.), poliskyb@sirna.com (B.P.)
[3]These authors contributed equally to this work.
[4]Present address: Intermune, Inc., 3280 Bayshore Boulevard., Brisbane, California 94005.
[5]Present address: Replidyne, Inc., 1450 Infinite Drive, Louisville, Colorado 80027.

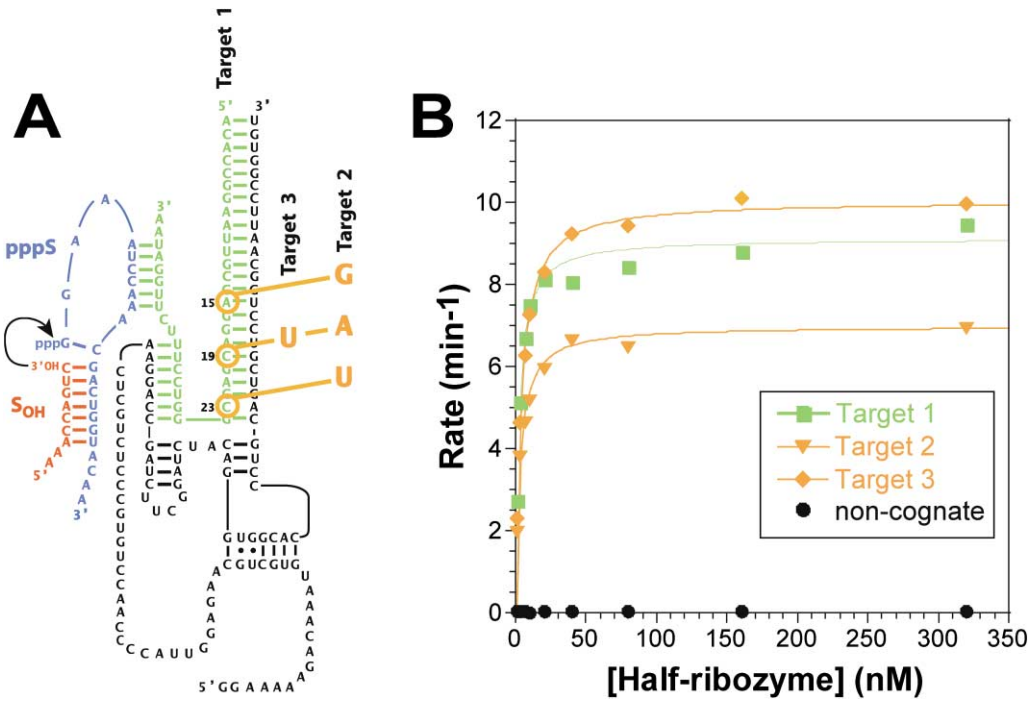

Figure 1. A Half-Ribozyme Activated by Natural Sequence Variants of HCV

(A) Half-ribozyme (black) interacts with a conserved sequence of the HCV genome (green). A S_{OH}/pppS bimolecular substrate RNA complex (red and blue, respectively) interacts with the half-ribozyme-HCV target complex by forming base pairs with the HCV target. The target-activated half-ribozyme catalyzes the ligation of S_{OH} and pppS by directing nucleophilic attack of the 3′-*cis*-diol of S_{OH} on the α-phosphate of pppS (arrow). Circled nucleotides in the target are sites of changes in the second and third most common variations of this sequence, targets 2 and 3, respectively. Relative to the consensus sequence, target 2 carries three changes at positions 15, 19, and 21, and target 3 contains a single C to U transition at position 19.

(B) Half-ribozyme catalysis with natural variants of the HCV target. Multiple turnover ligation rates were measured in the presence of a trace concentration of targets 1–3 and increasing concentrations of half-ribozyme. Rates with targets 1–3 and an unrelated target RNA of a different half-ribozyme are shown as green squares, orange triangles, orange diamonds, and black circles, respectively. The concentration of half-ribozyme was varied between 1 and 320 nM as shown, and the S_{OH} and pppS RNAs were present at 10 μM.

We assessed the ability of each of these three HCV targets to activate half-ribozyme catalysis. Since these three targets are expected to have differing affinities for the half-ribozyme, the target binding region of the half-ribozyme was extended by 13 nucleotides relative to the half-ribozyme described previously [1] in order to maximize capture of all targets at the lowest possible half-ribozyme concentration (Figure 1A). (Note: this extension does not alter the kinetic performance of the HCV half-ribozyme; data not shown). For each target, the maximal half-ribozyme rate (k_{max}) and apparent binding constant (K_{app}) were determined by monitoring the ligation rate as a function of half-ribozyme concentration in the presence of a trace amount of target (Figure 1B). The apparent binding constant for each of the HCV-target variants was less than or equal to 4 nM (Figure 1B). This result suggests that the half-ribozyme has a similar affinity for each target sequence, and that each sequence will be quantitatively bound in experiments used to detect and quantify HCV nucleic acid, which are performed at 1 μM half-ribozyme. Moreover, the very low apparent binding constants suggest that the half-ribozyme may be able to bind more divergent HCV-target sequences in these assays.

Since all of the target sequences have similar apparent binding constants, which are well below the half-ribozyme concentration used in assays to detect trace target, the amount of product formed in response to each target will be determined by the maximal rate it affords the half-ribozyme. The maximal rates afforded by target 1 and target 3 were similar (10.0 min^{-1} versus 9.1 min^{-1}, respectively), but target 2 elicited a $\sim$30% lower rate (7.0 min^{-1}). This result suggests that the HCV half-ribozyme will have a similar ability to detect each of the three targets. Thus, in so far as the 1431 entries in GenBank reflect the natural variation of the target in HCV 5′-UTR, the half-ribozyme can serve as a detection reagent for $\sim$80%, and possibly more, of reported HCV strains.

In contrast to the very similar kinetic performance of targets 1–3, a non-HCV RNA that serves to activate a distinct half-ribozyme [1] failed to activate catalysis of the HCV-activated half-ribozyme at any half-ribozyme concentration tested (Figure 1B and data not shown). The specificity of the HCV-activated half-ribozyme emphasizes that, like other target-activated ribozymes [13, 14], half-ribozyme activity relies on the ability of the target both to bind and to orient active site residues for catalysis. While it is unlikely that the non-HCV sequence in Figure 1B does either, the lower k_{max} observed with target 2 may reflect a perturbation in the structure of the target-half-ribozyme complex. Of the three nucleotide

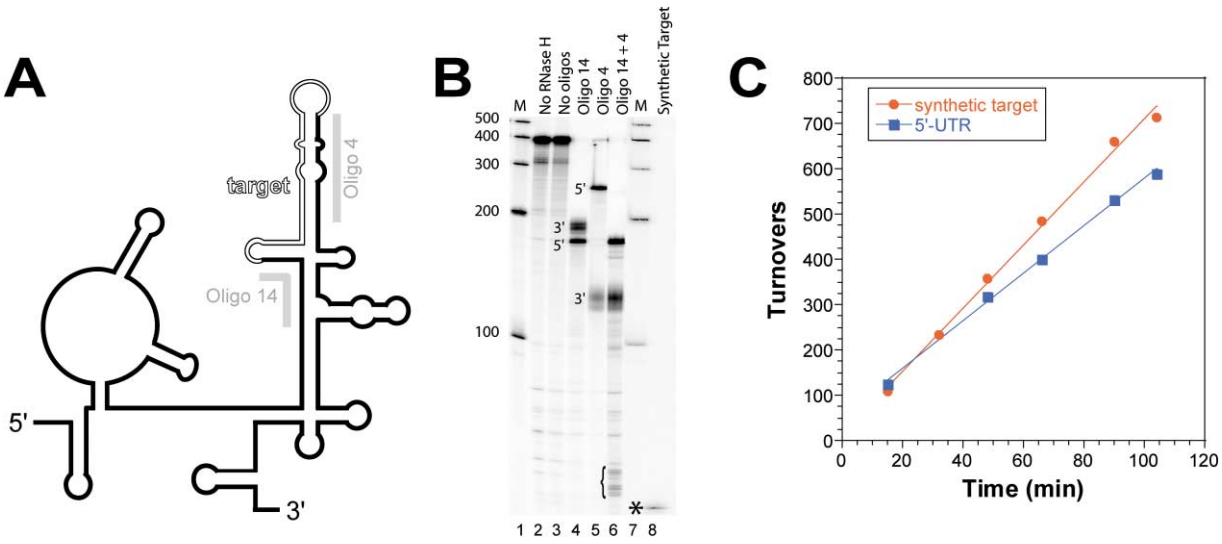

Figure 2. Half-Ribozyme Activation by Structured RNAs

(A) HCV 5′-UTR. DNA oligonucleotides (gray) used to direct RNase cleavage of the 5′-UTR are complementary to the sequences that flank the location of the HCV target (outline).

(B) Cleavage of radiolabeled 5′-UTR. Lanes 1 and 7, RNA markers; lanes 2–6, 5′-UTR treated as indicated; lane 8, synthetic target. The 5′ and 3′ cleavage products produced by RNase H cleavage of the 5′-UTR in the presence of oligonucleotides 4 and 14 are indicated (left of lanes 4 and 5, respectively). Synthetic target (asterisk) and targets derived from 5′-UTR (bracket) are indicated (left of lanes 8 and 6, respectively).

(C) Half-ribozyme turnover rate in the presence of an equal molar amount of synthetic target (circles) or 5′-UTR treated with RNase H and oligonucleotides that flank the target (squares). Reactions were performed in the presence of 1 μM half-ribozyme, 10 μM S_{OH} and pppS, and 1 nM synthetic target 1 or RNase H-cleaved 5′-UTR.

changes that could be responsible for this reduced rate, we note that a change at position 23 (Figure 1A) results in the formation of a canonical Watson-Crick pair at the site of a C/A mismatch that was a conserved feature of all half-ribozymes produced through iterative RNA selection and is present in targets 1 and 3 [1].

An Activator Derived from a Structured RNA

The target sequence is part of the 5′-UTR of HCV, a compact RNA structure [15] that directs cap-independent translation within cells [16]. The 5′-UTR displays a conserved secondary structure that forms independently of the remaining portion of the HCV genome [15, 17]. Since the target is sequestered in an intramolecular duplex within this structure, it was not surprising that an in vitro transcript comprising the intact 5′-UTR did not stimulate half-ribozyme catalysis (data not shown). Therefore, a strategy was devised to liberate the RNA target from the 5′-UTR such that it could activate the half-ribozyme.

To access the target within the structured 5′-UTR, it was treated with RNase H and DNA oligonucleotides that are complementary to the sequences that flank the target site (Figure 2A). After confirming that the UTR remains intact in the presence of RNase H without complementary oligonucleotides (compare lane 3 with lane 2, Figure 2B), we demonstrated that addition of a single oligonucleotide complementary to sequence either 5′ or 3′ of the target site cleaved the 5′-UTR to 100% and generated fragments of the expected sizes (lanes 4 and 5, respectively, Figure 2B). As expected, addition of both oligonucleotides to RNase H reactions resulted in cleavage at both sites and generated a set of products that are approximately the same size as the synthetic target shown in Figure 1A (compare bracket in lane 6 to the synthetic target in lane 8, Figure 2B). Thus, RNase H treatment can be used to efficiently produce fragments of the HCV 5′-UTR from in vitro transcripts that are approximately the same size as synthetic target 1.

To determine whether the RNA fragments generated by RNase H digestion of the 5′-UTR activate half-ribozyme catalysis, we measured multiple turnover rates in the presence of an equal amount of target 1 or the 5′-UTR cleaved in the presence of oligonucleotides that flank the target site. The observed rates are similar (7.4 min^{-1} versus 5.4 min^{-1}, respectively; Figure 2C). Thus, not only can RNase H treatment liberate RNA fragments from the 5′-UTR that resemble the synthetic target, but most if not all of these fragments activate half-ribozyme catalysis to the same extent as the synthetic oligonucleotide species. Because the 5′-UTR is likely to adopt the same structure when embedded in the viral genome [18], these data suggest that this half-ribozyme is competent to detect the HCV genome derived from live virus when integrated with an optimized method for clinical sample preparation.

Flexibility in Assay Formatting

Half-ribozyme activity can be detected directly by monitoring ligation of a radiolabeled substrate RNA on denaturing polyacrylamide gels ([1], Figures 1B and 2C). However, such assays are laborious and time consuming because they require separate steps for fractionation of product from unreacted substrate and detection and quantification of signal using phosphorimage analysis. Since both substrate RNAs can be chemically modified

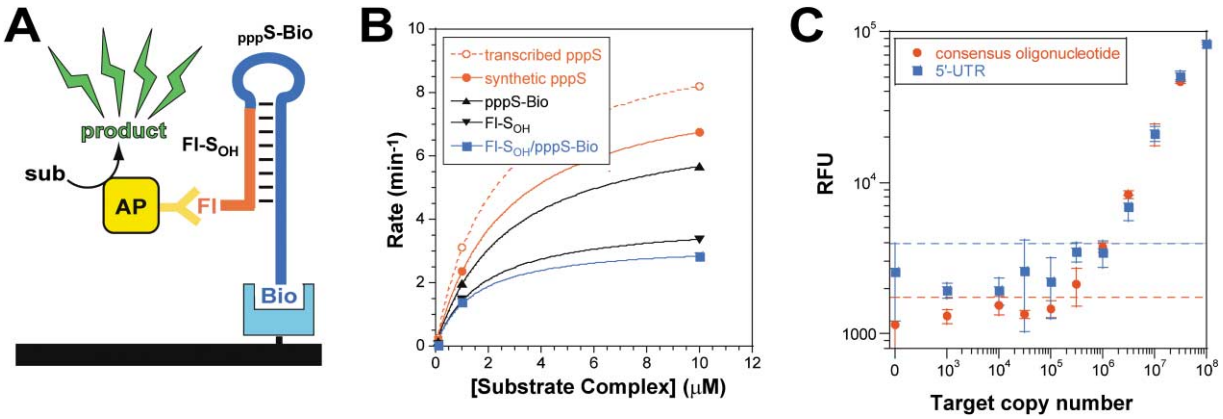

Figure 3. Detection of Half-Ribozyme Activity in ELISA-like Format

(A) Assay schematic. S_{OH} RNA was modified with a 5′-fluorescein moiety (Fl-S_{OH}, red), and a 3′-biotin tag was added to pppS (pppS-Bio, blue). The product was captured on streptavidin-coated 96-well plate and detected with an alkaline phosphatase-conjugated anti-fluorescein antibody (yellow). The alkaline phosphatase conjugate provides secondary signal amplification by converting a modified substrate into a fluorescent product that can be readily quantified.

(B) Kinetic performance of the fluorescein- and biotin-modified substrates. The multiple turnover ligation rates for substrate RNA combinations are indicated: S_{OH}/transcribed pppS (open circles), S_{OH}/synthetic pppS (closed circles), S_{OH}/pppS-Bio (upward triangles), Fl-S_{OH}/transcribed pppS (downward triangles), and Fl-S_{OH}/pppS-Bio (squares). Assays were performed at a half-ribozyme concentration of 1 μM and 0.1–10 nM target 1. S_{OH} and pppS were present in equimolar concentrations of 0.1–10 μM (as shown) and were always 1000-fold above the target concentration.

(C) Sensitivity of the half-ribozyme for synthetic HCV target and RNase-cleaved HCV 5′-UTR in the ELISA-like format. Five replicate half-ribozyme reactions were carried out for each amount of HCV target (0–1 × 10^8), and ligation products were quantified by ELISA-like detection as described in Experimental Procedures. Average signal plus one standard deviation in absence of target 1 (dashed red line) or 5′-UTR (dashed blue line) are indicated. Note that the S_{OH} and pppS sequences used in these experiments are optimized versions of those shown in Figure 1A; the sequences of these substrate RNAs can be found in Experimental Procedures.

(labeled) during their synthesis with moieties employed in high-throughput detection assays, we set out to integrate half-ribozyme-mediated signal amplification with more convenient assay formats.

ELISA-type assays have found application from basic research to clinical diagnostics because the ELISA format allows for detection and quantification of analytes in a nonradioactive, easy-to-use format that can be automated. ELISA assays require both capture and detection steps and are usually performed in a microtiter plate. The ability to synthesize one half-ribozyme substrate with a capture agent and the second substrate RNA with a hapten for antibody detection provided a potential route to detect half-ribozyme catalysis in an ELISA-like format (Figure 3A). To facilitate capture of the ligation product, a biotin tag was introduced on the 3′ end of the 3′-substrate RNA (pppS-Bio; see Experimental Procedures for chemical synthesis of 5′-triphosphorylated RNAs). A fluorescein moiety, introduced at the 5′ end of the 5′ substrate RNA (Fl-S_{OH}), allowed for detection of the captured product. This moiety can be detected directly upon ligation (data not shown) or indirectly following a secondary signal amplification step using an anti-fluorescein antibody conjugated to alkaline phosphatase (Figure 3A). The latter protocol involves binding the reaction products to a streptavidin plate, washing under denaturing and then native conditions, binding and washing away excess anti-fluorescein antibody-enzyme conjugate, and addition of an alkaline phosphatase substrate that is converted by an enzymatic reaction to a fluorescent product. The advantage of this system over the direct detection of radiolabeled products fractionated by gel electrophoresis is in its speed and simplicity. The washing and buffer addition steps can be accomplished by multichannel pipets or using a robotic liquid handling station. Results from a 96-well ELISA-like assay can be obtained with a fluorescent plate reader 20 min after the addition of the alkaline phosphatase substrate.

Prior to developing ELISA-like detection of half-ribozyme ligation product, the kinetic performance of the half-ribozyme with the pppS-Bio and Fl-S_{OH} substrate RNAs was examined using radiolabeled substrates in a standard gel-based assay (Figure 3B). Because pppS-Bio was prepared by enzymatic ligation of a chemically triphosphorylated oligonucleotide to a biotin-containing RNA, we first compared nonbiotinylated pppS prepared in this fashion to an in vitro-transcribed pppS preparation. The chemically synthesized pppS shows a minor reduction in ligation rate relative to pppS produced by T7 RNA polymerase transcription (Figure 3B, open versus closed circles). While the addition of a 3′-biotin moiety has an additional effect on the ligation rate (upward black triangles, Figure 3B), the overall effect of exchanging the transcribed pppS for a synthetic 3′-biotinylated pppS is relatively small (less than 2-fold in k_{max}; Figure 3B). The introduction of a fluorescein on the 5′ end of S_{OH} has a greater impact on the ligation rate (4-fold in k_{max}). We observed that the rate reductions observed with these modified substrates are not additive, and the Fl-S_{OH} performs similarly with either transcribed pppS or chemically synthesized pppS-Bio. Thus, relative to the unmodified substrate RNAs used in a previous study, those developed for ELISA-like formatting slightly im-

pede half-ribozyme catalysis, and therefore were expected to compromise the sensitivity of target detection when half-ribozymes were used in an ELISA-like format based on a model that predicts sensitivity of detection from kinetic properties [1].

To directly investigate assay sensitivity in the ELISA-like format, half-ribozyme ligation reactions were carried out with increasing amounts of synthetic HCV target or RNase H-digested 5′-UTR (n = 5). The ligation product was captured on a streptavidin-coated 96-well plate and detected with an antibody coupled to alkaline phosphatase. As expected based on kinetic studies with RNase H-cleaved HCV 5′-UTR (Figure 1C), the signals observed in the presence of target 1 or RNase H-digested 5′-UTR were similar when signal was appreciably above background. When target 1 (synthetic oligoribonucleotide) was used to activate the half-ribozyme, 1×10^6 target molecules (1.6 attomol, 330 fM) produced a signal distinct from that in the absence of target by one standard deviation (red circles, Figure 3C). At lower amounts of target, signal reached a plateau at the level observed in the absence of target. Similarly, RNase H-digested 5′-UTR provided a signal above background at 3×10^6 target molecules (5 attomol, 1 pM) (blue squares, Figure 3C). The ability of the half-ribozyme to equally detect 3×10^6 copies of a synthetic target oligonucleotide or a sequence derived from the intact HCV 5′-UTR represents at least a 6000-fold improvement in sensitivity relative to the next most sensitive ribozyme-based detection strategy, which required RT-PCR amplification for detection of an unstructured DNA [6].

As predicted from earlier studies that established the sensitivity of the HCV-activated half-ribozyme using radiolabeled substrate RNAs [1], the sensitivity of the ELISA-like assay is dictated in part by the target-independent ligation reaction (i.e., the signal observed in the absence of target). In the ELISA-formatted assay, this target-independent reaction produces a signal equivalent to that observed in the presence of approximately 1×10^5 target molecules (Figure 3C); this background signal is approximately 10-fold higher than the signal observed when the substrate RNAs are added to the streptavidin plate without prior incubation either in the presence or the absence of half-ribozyme (80–200 RFU; data not shown). We previously demonstrated that the background reaction is not catalyzed by the half-ribozyme, but rather represents the intrinsic reactivity of the S_{OH}/pppS substrate complex [1].

Detection on Optical Surfaces

Optical immunoassays (OIA) have previously been used to detect nucleic acid targets [19, 20]. Existing OIA assays use an immobilized antisense probe to capture a target nucleic acid on the surface of a silicon wafer. A second antisense probe carrying biotin interacts with a different sequence in the target, and the biotin moiety is then detected using a horseradish peroxidase-avidin conjugate that converts a soluble substrate into an insoluble product. Local deposition of the product on the atomically flat silicon wafer changes the optical thickness of the surface. The change in optical thickness results in destructive interference at certain wavelengths of light and a change in surface color. This system was designed to exploit the ability of the human eye to discriminate changes in color more readily than intensity differences. The ability to assess results visually without instrumentation has enabled the production of diagnostic assays that run in a physician's office without sophisticated instrumentation. Quantification of signal using a CCD camera to generate a color difference value allows assays to be run in a high-throughput microplate format. In previous studies, product detection by the OIA method was 5×10^6-fold more sensitive than similarly formatted fluorescence detection methods using a CCD detection strategy [19].

We adapted this assay to detect half-ribozyme product RNA (Figure 4A). For this application, substrate RNAs were designed such that S_{OH} carried a 5′-biotin (Bio-S_{OH}) and the 3′ end of pppS was extended by 17 nucleotides to facilitate hybrid capture (pppS-Ext). Half-ribozyme product RNA is captured by an immobilized antisense oligonucleotide, and the 5′-biotin label is detected using a peroxidase-avidin conjugate. To avoid detection of unligated Bio-S_{OH} annealed to pppS-Ext, a competitor oligonucleotide that binds to the entire portion of pppS-Ext that does not interact with the capture oligonucleotide was used to abrogate its ability to form base pairs with Bio-S_{OH} (Figure 4A).

Kinetic characterization of the Bio-S_{OH}/pppS-Ext substrate pair in analogy to the analysis of the substrate RNAs used in the ELISA-like assay indicated that Bio-S_{OH} and pppS-Ext reduce maximal half-ribozyme rate by roughly 4-fold relative to the originally reported substrate RNAs (data not shown). The rate reduction relative to the unmodified RNAs is similar to that observed with substrate RNAs used in ELISA-like assays. In this case, however, the kinetic defect was primarily attributed to the 3′ substrate RNA (pppS-Ext) rather than the 5′ substrate RNA (Bio-S_{OH}).

As predicted from the kinetic equivalence of half-ribozyme catalysis using substrate RNAs formatted for the OIA and ELISA-like assays, the sensitivity of detection of the synthetic oligoribonucleotide target (target 1) in OIA-formatted half-ribozyme reactions is similar to that observed in ELISA-formatted reactions (compare Figure 3C to Figures 4B and 4C). In both assays, signal separated from background by one standard deviation is evident at 1×10^6 target molecules (1.6 attomol, 330 fM) and reached a plateau at lower amounts of target 1. In the OIA assay, a transition between the background gold color and positive blue is observed at this target level (Figure 4B). In the quantified data, the signal from 1×10^6 target molecules is clearly above the average background signal observed in reactions containing 0 to 1×10^5 target molecules (Figure 4C). As with the ELISA-like format, half-ribozyme-mediated detection is at least 6000-fold greater than the maximal reported sensitivity of other nucleic acid-activated ribozymes [6].

Sensitivity of Detection

The sensitivity of detection provided by ELISA-like and OIA-formatted half-ribozyme reactions is similar to the sensitivity of protein detection provided by standard immunoassays. Immunological assays for protein de-

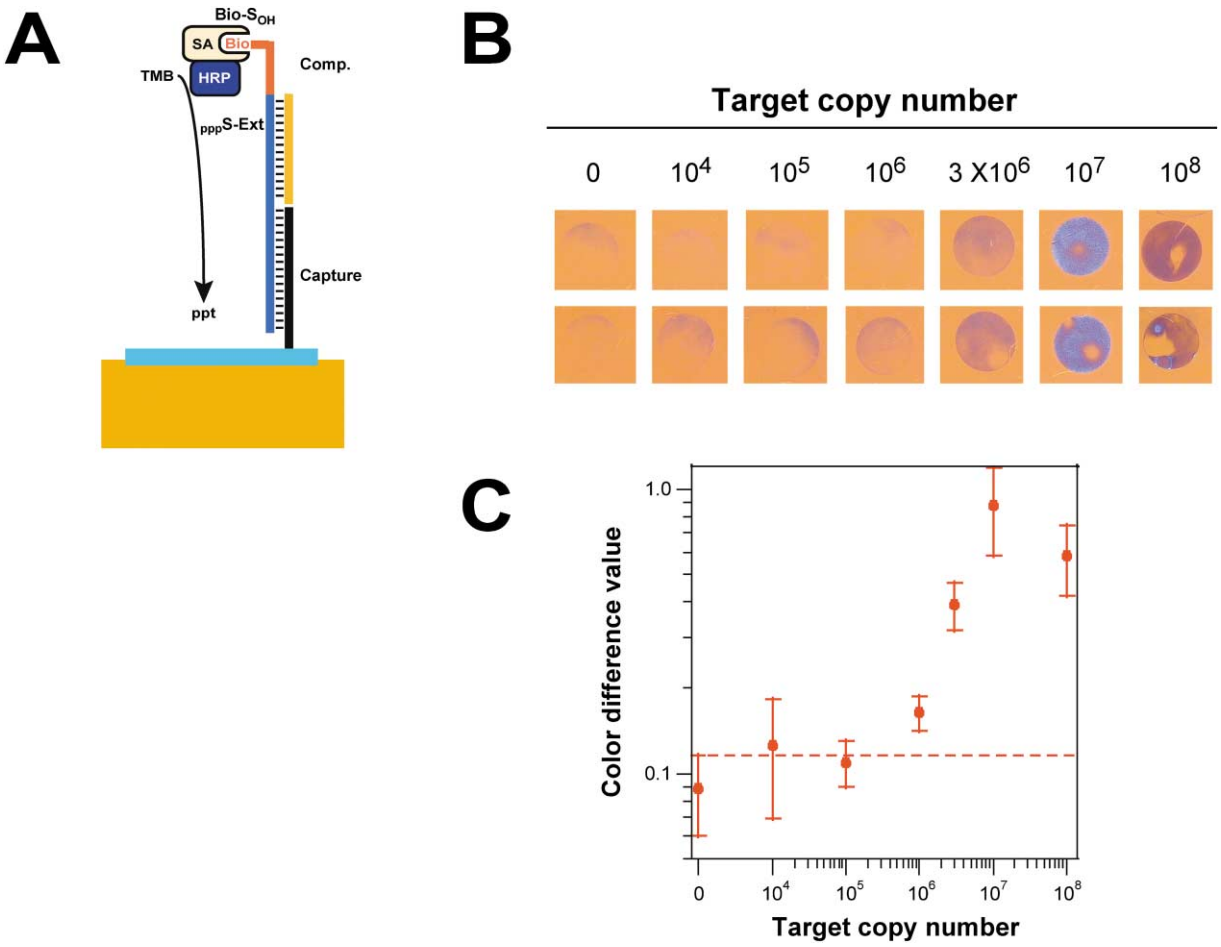

Figure 4. Detection of Half-Ribozyme Activity on Optically Coated Silicon Wafers

(A) The optical immunoassay format employs an extended pppS (blue) that is captured by a hybridization probe (black) immobilized on the surface of the silicon wafer (gold). The S_{OH} RNA (red) carries a 5′-biotin moiety, which allows captured half-ribozyme ligation product to bind a steptavidin-horseradish peroxidase conjugate (SA-HRP) that converts a soluble substrate (TMB) into an insoluble product. Localized precipitation of the product leads to the deposition of a thin film on the suface of the wafer, which alters the optical thickness of the surface and changes the color of the wafer. To eliminate background caused by the annealing of unligated Bio-S_{OH} to the to the captured pppS-Ext, a DNA oligonucleotide (tan) was added to compete for binding to the complementary sequence.

(B) Visual detection of half-ribozyme product RNA using the optical immunoassay format. Half-ribozyme reactions were carried out with increasing amounts of HCV target (0–1 $\times$ 10^8), and the products were detected on silicon wafers as described in Experimental Procedures. In the absence of product deposition, the plate is gold. Localized product precipitation shifts the color of the plate to a purple/blue hue that is apparent at $\geq$ 1 $\times$ 10^6 target molecules. As the thickness on the surface increases with increasing amounts of ligation product detected, surface color transitions from gold to purple, from purple to blue, and then from blue to white. As surface thickness increases even further, the color will transition back from white to blue due to the periodic nature of light. Consequently, signal at 1 $\times$ 10^8 target molecules appears lower than signal at 1 $\times$ 10^7 target molecules.

(C) Quantification of data from panel B was performed using a CCD camera and plotted as a function of HCV target amount (see Experimental Procedures). Average signal plus one standard deviation in absence of target 1 (dashed red line) is indicated.

tection have a calculated theoretical maximum limit of detection of 20 fM to 0.2 fM based on typical antibodies with affinities of 10^{-9} M to 10^{-11} M, respectively [21]. In practice, however, highly sensitive standard immunoassays have limits of detection of 35 to 700 fM [22, 23]. By comparison, half-ribozymes display a sensitivity of detection in both ELISA-like and OIA-like assays of ~330 fM (1 $\times$ 10^6 molecules) of an unstructured HCV target RNA or (Figures 3C and 4C) or ~1 pM (3 $\times$ 10^6 molecules) of the 5′-UTR of HCV (Figure 3C).

Even though half-ribozymes are currently comparable to immunoassays in sensitivity, greater sensitivity may be possible. The sensitivity of detection of the synthetic target oligonucleotide by half-ribozymes in the assays reported here is diminished approximately 140-fold relative to that reported in an assay that directly monitored radiolabeled product RNA (~1 $\times$ 10^6 molecules, Figures 3C and 4C, versus ~7000 molecules, [1]). The differing sensitivity in ELISA-like and OIA formats is largely a consequence of how sensitivity is defined here (separation of target signal and control signal by one standard deviation) relative to the prior study (intersection of regressed signal as a function of target concentration with signal value in absence of target). The large CV observed

in the absence of target and in the presence of low levels of target in both ELISA-like and OIA assays (~51% and 31%, respectively, in the absence of target) results in a higher limit of detection in these assays. These high CVs are not intrinsic to half-ribozyme catalysis, since the coefficient of variance (CV) is less than 8% in assays that monitor radiolabeled product RNA directly [1]. Therefore, efforts to minimize data scatter through further assay development could dramatically improve sensitivity in both ELISA-like and OIA formats.

Following a model that predicts the sensitivity afforded by half-ribozymes from the ratio of target-activated catalysis and background ligation [1], we attribute a smaller part of the reduced sensitivity of the ELISA-like and OIA-formatted assays to the diminished catalytic performance of the half-ribozyme when utilizing modified substrate RNAs (Figure 3B and data not shown). Consequently, optimization of the utilization of the modified substrate RNAs by the half-ribozyme should improve sensitivity in either assay format. This improvement in utilization could be realized either by "training" half-ribozymes to use modified substrate RNAs through iterative RNA selection or by screening substrate RNAs for positions where modifications are best tolerated. Through a combination of assay and half-ribozyme performance improvements, further gains in the sensitivity afforded by half-ribozymes in immunodiagnostic assays can be expected.

Current screening for HCV infection is performed through the detection of anti-HCV antibodies [24, 25]. However, this approach cannot distinguish individuals who are actively infected from those who have cleared the virus and reports recently infected individuals who have yet to seroconvert as HCV negative [24, 25]. To address these deficits, detection of HCV antigens has been added to screening procedures, but the hypervariability of viral proteins limits the ultimate effectiveness of this approach [24]. Nucleic acid-based detection methods, such as polymerase chain reaction (PCR) and transcription mediated amplification (TMA), have demonstrated a superior solution to these challenges because they detect only active infections, can be directed to the most highly conserved portions of the HCV genome, and offer greater sensitivity than immunological methods [25]. However, the high cost of these methods has limited their application in blood screening [26]. The half-ribozyme system that we report here has a current sensitivity of detection similar to immunological methods used to detect viral contamination of blood products, but offers the other benefits of nucleic acid-testing methods while retaining the high throughput and lower cost of immunoassays.

Significance

Several authors have discussed the potential use of target-activated ribozymes in clinical diagnostic applications [27–29], and we previously developed a ribozyme system capable of detecting low-abundance nucleic acids [1]. The current work supports the prospect of using ribozyme-based systems to monitor viral nucleic acids by demonstrating that (1) the half-ribozymes can detect natural HCV sequence variants, (2) a half-ribozyme can detect its target when derived from a structured RNA, and (3) half-ribozyme-based signal amplification can be integrated with two immunoassay detection platforms. Although the sensitivity of detection afforded by ELISA and OIA formats remains to be optimized, the sensitivity in the assays reported here is equivalent to that provided by immunological methods currently used as primary screens for viral contamination of blood products. Together, these properties suggest that ribozyme-based reagents like the one described here may prove useful for viral screening and for other diagnostic applications.

Experimental Procedures

RNA Sequences and Preparation

The S_{OH} RNAs and synthetic HCV target RNAs shown in Figure 1A and the "noncognate" RNA used in Figure 1B (5′-ACACCGGAA UUGCCAGGACGACCGGGUCCUUUCUUGGAUAA) were produced through standard oligoribonucleotide synthesis procedures. Nonbiotinylated pppS RNAs were prepared by T7 RNA polymerase transcription; pppS carrying a 3′-biotin was made by chemical modification of synthetically produced oligonucleotides as described below. The half-ribozyme shown in Figure 1A was used in all experiments and was produced by T7 RNA polymerase transcription using a template produced by PCR amplification of a cloned ribozyme sequence [1] with appropriate primer sequences. The HCV 5′-UTR (nt 1–397) was produced by run-off transcription of a restriction endonuclease-digested plasmid template carrying a portion of the HCV genome under the control of a T7 promoter. Substrate RNAs used in ELISA-like and OIA-like assays were modified versions of the sequences shown in Figure 1A. The sequences of these substrates are as follows: Fl-S_{OH} (5′ fluorescein-AAACCAGUG), pppS-Bio (GGAAGUCUAAACCACUGGUACAA-biotin), Bio-S_{OH} (5′ biotin-AAACCAGUG), and pppS-Ext (5′-GGAAGUCUAAACCACUGGUA CAAGCGUAACUCUGUCGAUCG).

Synthetic pppS RNAs were produced by splint-directed ligation of the chemically triphosphorylated sequence pppGGAAGU to the remaining portion of pppS using T4 DNA ligase [30]. The 5′-triphosphorylated oligonucleotide was prepared by subjecting a solid support-bound oligonucleotide to a modified procedure used for the preparation of nucleoside 5′-triphosphate [31] as described below.

The oligonucleotide (GGAAGU) was synthesized on controlled pore glass (CPG) beads on a 100 μmole scale using standard phosphoramidite chemistry. Approximately one-half of this synthesis was dried under vacuum in a synthesis column for 2 hr at 35°C. The column was washed with 20 ml dry pyridine followed by 20 ml dry DMF and 10 ml dioxane-pyridine-DMF (6:3:1). A freshly prepared solution of salicyl chlorophosphite (2.03 g) in dioxane (8 ml) was slowly pushed through the column over the course of 20 min. The column was then washed with 20 ml dioxane followed by 20 ml acetonitrile. A well-mixed solution of 0.5 M $P_2O_7^{4-}$·1.5 Bu_3N (2.28 g, Sigma-Aldrich, Inc.) in 9 ml DMF-Bu_3N (6.2:1) was then slowly pushed through the column for 20 min. The column was then washed with 20 ml dry DMF followed by 20 ml acetonitrile. Ten milliliters of oxidation solution (3g I_2 in H_2O-pyridine-THF 2:20:75 v/v) was pushed through the column for 30 min. The column was washed with 20 ml 70% pyridine-water, 20 ml acetonitrile, 20 ml THF, and dried under high vacuum at 35°C.

The CPG beads were removed from the column and treated with 10 ml of methylamine for 5 hr at 35°C. Solvents were then evaporated under vacuum. The resin was treated for 16 hr with 2 ml of 1 M TBAF (Sigma-Aldrich, Inc.). Prior to use, TBAF was dried for 3 days over activated 4A molecular sieves. The TBAF was quenched with 5 ml of 1.5 M sodium acetate (pH 5.2). THF was removed under vacuum, and the aqueous layer was extracted twice with ethyl acetate. The product pppRNA was precipitated with 20 ml of ethanol, centrifuged at 16000 × g, and purified via denaturing gel electrophoresis.

Kinetic Assays

The half-ribozyme kinetic assays were performed at 23°C in 30 mM Tris-HCl (pH 7.5), 160 mM $MgCl_2$, 700 mM KCl, and 0.6 mM EDTA. Half-ribozyme and substrate RNA concentrations used in each assay are provided in the appropriate figure legends. For gel-based kinetic assays (Figures 1B, 2C, and 3B), a trace amount of added substrate was radiolabeled. Either S_{OH} was radiolabeled using T4 polynucleotide kinase, or pppS was transcribed in the presence of α-[^{32}P]-GTP. Prior to each reaction, the half-ribozyme and target were refolded by heating at 80°C for 2 min., adding concentrated reaction buffer, and allowing the mixture to cool to 23°C over 5 min. Reactions were initiated by addition of substrate RNAs, and aliquots were quenched into formamide gel-loading dye containing 50 mM EDTA at the appropriate times. Products were resolved on 15% denaturing polyacrylamide gels. Observed turnover rates were calculated from the initial phase of the reaction (<20% substrate converted to ligated product) and fit to k_{obs}= [ligated product]/([target-half-ribozyme]*time). Michaelis-Menten parameters were established by varying concentration of half-ribozyme in the presence of trace target, and the data were fit to $v = [E^*][E]k_{max}/(K_{app}+[E])$, where v equals rate at each [E], [E*] represents the concentration of active half-ribozyme (defined as the concentration of target), K_{app} is the half-ribozyme concentration required for half-maximal activation, and k_{max} equals the maximal catalytic rate. For assays in which the concentration of active half-ribozyme ([E*], defined by the limiting target concentration) was fixed and the concentration of RNA substrate complex varied (e.g., Figure 3B), the substrate concentration ([S]) replaces [E] in the equation above, and K_{app} is the substrate concentration required for half-maximal activation.

RNase H Digestions

Reactions for the oligonucleotide-directed RNase digestion of HCV 5′-UTR (nt 1–397) were carried out in a 5 μl reaction containing 20 mM Tris (pH 7.5), 100 mM KCl, 10 mM $MgCl_2$, 0.1 mM DTT, 0.5 units RNase H (Roche), 1 μM DNA oligonucleotide, and varying concentrations of target RNA. To assist in the annealing of the DNA oligonucleotides, the RNA target and targeting DNAs were heated at 95°C for 5 min in Tris and KCl and allowed to cool to room temperature prior to the addition of the remaining buffer components and RNase H. Reactions were performed at 37°C for 30 min. The products were ethanol precipitated, washed with 70% ethanol, resuspended in 2.5 μl of water, and used directly in half-ribozyme ligation reactions.

ELISA-like Detection

Sensitivity determinations (n = 5) were carried out at 23°C in 30 mM MES (pH 6.0), 0.7 M KCl, 160 mM $MgCl_2$, 0.6 mM EDTA, 1 μM half-ribozyme, 1 μM Fl-S_{OH}, and 1 μM pppS-Bio. The HCV target, either synthetic target or RNase H-cleaved 5′-UTR, was present at 0 or 1×10^3–1×10^8 molecules per reaction. The final reaction volume was 5 μl. Target stocks at appropriate concentrations were prepared by serial dilution of a concentrated stock into 100 ng/μl yeast tRNA. The diluted HCV-UTR was treated with RNase H, ethanol precipitated, and redissolved in water as described above. An individual RNase H reaction was performed for each half-ribozyme assay, and the concentration of RNase H-cleaved HCV-UTR in each assay is the amount of target in the initial RNase H reaction. Reactions were assembled as described for the kinetic assays above and run for 19 hr. The reaction was then diluted in 100 μl binding buffer (PBS: 20 mM phosphate [pH 7.5], 150 mM NaCl) and transferred to a 96-well steptavidin-coated microtiter plate (Amersham Pharmacia, Inc.) that had been prewashed with 3× 200 μl Tris-buffered saline (TBS: 25 mM Tris-HCl [pH 7.2], 150 mM NaCl). The plate was covered and incubated on a shaker for 1 hr. The product was removed, and the plate was washed with 3× 200 μl of TBS plus 7 M urea, then 3× 200 μl TBS plus 0.1% Tween-20. Note that background associated with the annealing of unligated Fl-S_{OH} to the immobilized pppS-Bio substrate through Watson-Crick base pairing was reduced/eliminated via the denaturing washes. One hundred microliters of an alkaline phosphatase-conjugated anti-FITC antibody (Boehringer Mannheim, Inc.) diluted 1:5000 in SuperBlock Buffer (Pierce) was added, and the reaction was incubated for 30 min on a shaker. Unbound conjugate was removed by washing with 3× 200 μl TBS plus 0.1% Tween-20, and 100 μl of AttoPhos substrate (Boehringer Mannheim, Inc.) was applied. Following a 20 min reaction at room temperature, the results were quantified on an Applied Biosystems Cytofluor series 4000 fluorimager.

OIA Detection

Surface Preparation

Details of the preparation of the optically coated silicon wafers were described previously (18). Briefly, Si_3N_4 was applied to crystalline silicon wafers in a vapor deposition chamber. The polymer, T-structure aminoalkyl poly-dimethyl siloxane (TSPS; United Chemical Technologies) was applied using a spin coater and cured at 150°C for 24 hr to create a thin film biosensor surface. An amino-functionalized surface (TSPS/PPL) was prepared by passively adsorbing 5 μg/ml of poly (lys-phe) (Sigma, St. Louis, MO) in 1× PBS, 2M NaCl (pH 6) overnight at room temperature. The TSPS/PPL wafer was diced into 49 mm^2 chips using a scribe/break robot as described elsewhere [18].

Probe Immobilization

Oligonucleotides were synthesized with a 5′ amino modifier C6 phosphoramidite (Glen Research), resuspended in water, and stored at –70°C until further use. The capture probe (5′-XYCGATCGACA GAGTTACGCTTGT-3′, where X = C_6 amine amidite and Y = C_{18} spacer amidite) was dried and resuspended in 5 μl of 0.1M TEAA (pH 7.8). Disuccinimidyl suberate (Pierce) was dissolved to 28 mg/ml in dimethyl formamide (Aldrich), and 22 μl was added to the capture probe and incubated at room temperature for 10 min. Ice-cold water was added (200 μl), followed by three extractions with 600 μl of ethyl acetate (Aldrich). Ice-cold water was added (200 μl), and the sample was extracted twice with 400 μl of iso-butyl alcohol (Aldrich). Probes were resuspended to 500 μl in ice-cold water and placed on ice. The probe was resuspended to 150 nM in 0.1 M phosphate buffer (pH 7.8), and 15 μl was applied to each chip. The probe spot was incubated in a humid environment for 2 hr. The chip surface was washed thoroughly with water and then "stripped" of passively adsorbed material with 0.1% SDS at 53°C for 2 hr. The chip was then washed again with water, dried under a nitrogen stream, and stored in a N_2 box until further use.

Assay Protocol

Sensitivity determinations (n = 4) were carried out at 23°C in 30 mM MES (pH 6.0), 0.7 M KCl, 160 mM $MgCl_2$, 1 μM half-ribozyme, 1 μM Bio-S_{OH}, and 1 μM pppS-Ext. The HCV target was present at 0 or 1×10^4–1×10^8 molecules per reaction. Half-ribozyme products (5 μl) were mixed with 5 μl of 7 mM competitor (5′-ACC AGT GGT TTA GAC TTC C-3′) and diluted with 45 μl hybridization solution (5× SSC, 0.1% SDS, 0.5% BlockAid [Thermo Electron, Louisville, CO]). Following 2 min of heating at 70°C, samples (50 μl) were loaded on OIA chips. Hybridization was performed at room temperature for 30 min. Plates were then washed with wash buffer A (0.1% SDS/0.1× SSC) followed by wash buffer B (0.1× SSC). A conjugate solution, peroxidase-conjugated IgG fraction monoclonal mouse anti-biotin (Jackson Research), of 1 μg/ml (made in hybridization buffer) was added to each well (125 μl), and samples were incubated at room temperature for 10 min, followed by washing with wash buffer A, then by buffer B. TMB reagent (BioFX) was added (150 μl), and plates were incubated for 10 min at room temperature, then washed with ddH_2O. Chips were finally washed with methanol manually and dried upside down in a 65°C oven.

CCD Camera Quantitation

Individual chips were imaged using a SSC-DC54 CCD camera (Sony) with an illuminator (Dolan-Jenner Industries, Inc., Lawrence, MA). Images were quantified using Wit image processing software (Correco Inc., Quebec, Canada). The color change of the surface was quantified using a color difference relation as follows:

$$CD = \frac{((Rs - Rb)^2 + (Gs - Gb)^2 + (Bs - Bb)^2)^{1/2}}{(Rb + Gb + Bb)/3.}$$

The surface was divided into two areas, the background and the capture probe spot. The background was defined as the entire surface, whereas the capture probe spot was the area encompassing the capture probe. The software calculated the average readings

of red, green, and blue for the spot and the background, and these were designated Rs, Gs, Bs, and Rb, Gb, and Bb, respectively.

Acknowledgments

We thank members of Sirna Therapeutics, Inc. and Thermo Electron, Inc. for helpful discussions throughout the course of this work. Special thanks to Jasenka Adamic for advice on triphosphate RNA synthesis.

Received: January 27, 2004
Revised: March 22, 2004
Accepted: March 25, 2004
Published: June 25, 2004

References

1. Vaish, N.K., Jadhav, V.R., Kossen, K., Pasko, C., Andrews, L.E., McSwiggen, J.A., Polisky, B., and Seiwert, S.D. (2003). Zeptomole detection of a viral nucleic acid using a target-activated ribozyme. RNA *9*, 1058–1072.
2. Bartel, D.P., and Szostak, J.W. (1993). Isolation of new ribozymes from a large pool of random sequences. Science *261*, 1411–1418.
3. Ekland, E.H., and Bartel, D.P. (1995). The secondary structure and sequence optimization of an RNA ligase ribozyme. Nucleic Acids Res. *23*, 3231–3238.
4. Ekland, E.H., Szostak, J.W., and Bartel, D.P. (1995). Structurally complex and highly active RNA ligases derived from random RNA sequences. Science *269*, 364–370.
5. Bergman, N.H., Johnston, W.K., and Bartel, D.P. (2000). Kinetic framework for ligation by an efficient RNA ligase ribozyme. Biochemistry *39*, 3115–3123.
6. Robertson, M.P., and Ellington, A.D. (1999). In vitro selection of an allosteric ribozyme that transduces analytes to amplicons. Nat. Biotechnol. *17*, 62–66.
7. Porta, H., and Lizardi, P.M. (1995). An allosteric hammerhead ribozyme. Biotechnology (N. Y.) *13*, 161–164.
8. Komatsu, Y., Yamashita, S., Kazama, N., and Ohtsuka, E. (1999). Induction of ribozyme activity by anti-ribozyme oligonucleotides. Nucleic Acids Symp. Ser. *42*, 279–280.
9. Kuwabara, T., Warashina, M., and Taira, K. (2000). Allosterically controllable ribozymes with biosensor functions. Curr. Opin. Chem. Biol. *4*, 669–677.
10. Wang, D.Y., Lai, B.H., Feldman, A.R., and Sen, D. (2002). A general approach for the use of oligonucleotide effectors to regulate the catalysis of RNA-cleaving ribozymes and DNAzymes. Nucleic Acids Res. *30*, 1735–1742.
11. Burke, D.H., Ozerova, N.D., and Nilsen-Hamilton, M. (2002). Allosteric hammerhead ribozyme TRAPs. Biochemistry *41*, 6588–6594.
12. Iyo, M., Kawasaki, H., and Taira, K. (2002). Allosterically controllable maxizymes for molecular gene therapy. Curr. Opin. Mol. Ther. *4*, 154–165.
13. Vaish, N.K., Dong, F., Andrews, L., Schweppe, R.E., Ahn, N.G., Blatt, L., and Seiwert, S.D. (2002). Monitoring post-translational modification of proteins with allosteric ribozymes. Nat. Biotechnol. *20*, 810–815.
14. Hartig, J.S., Najafi-Shoushtari, S.H., Grune, I., Yan, A., Ellington, A.D., and Famulok, M. (2002). Protein-dependent ribozymes report molecular interactions in real time. Nat. Biotechnol. *20*, 717–722.
15. Kieft, J.S., Zhou, K., Jubin, R., Murray, M.G., Lau, J.Y., and Doudna, J.A. (1999). The hepatitis C virus internal ribosome entry site adopts an ion-dependent tertiary fold. J. Mol. Biol. *292*, 513–529.
16. Rijnbrand, R.C., and Lemon, S.M. (2000). Internal ribosome entry site-mediated translation in hepatitis C virus replication. Curr. Top. Microbiol. Immunol. *242*, 85–116.
17. Kieft, J.S., Zhou, K., Grech, A., Jubin, R., and Doudna, J.A. (2002). Crystal structure of an RNA tertiary domain essential to HCV IRES-mediated translation initiation. Nat. Struct. Biol. *9*, 370–374.
18. Tsukiyama-Kohara, K., Iizuka, N., Kohara, M., and Nomoto, A. (1992). Internal ribosome entry site within hepatitis C virus RNA. J. Virol. *66*, 1476–1483.
19. Jenison, R., Yang, S., Haeberli, A., and Polisky, B. (2001). Interference-based detection of nucleic acid targets on optically coated silicon. Nat. Biotechnol. *19*, 62–65.
20. Jenison, R., La, H., Haeberli, A., Ostroff, R., and Polisky, B. (2001). Silicon-based biosensors for rapid detection of protein or nucleic acid targets. Clin. Chem. *47*, 1894–1900.
21. Davies, C. (2001). Introduction to immunoassay priniciples. In The Immunoassay Handbook, D. Wild, ed. (London: Nature Publishing Group), p. 38.
22. Thonnart, B., Messian, O., Linhart, N.C., and Bok, B. (1988). Ten highly sensitive thyrotropin assays compared by receiver-operating characteristic curves analysis: results of a prospective multicenter study. Clin. Chem. *34*, 691–695.
23. McConway, M.G., Chapman, R.S., Beastall, G.H., Brown, E., Tillman, J., Bonar, J.A., Hutchison, A., Allison, T., Finlayson, J., and Weston, R. (1989). How sensitive are immunometric assays for thyrotropin? Clin. Chem. *35*, 289–291.
24. Majid, A.M., and Gretch, D.R. (2002). Current and future hepatitis C virus diagnostic testing: problems and advancements. Microbes Infect. *4*, 1227–1236.
25. Dufour, D.R. (2002). Hepatitis C: laboratory tests for diagnosis and monitoring of infection. Clinical Laboratory News *November*, pp. 10, 12, 14.
26. Conry-Cantilena, C. (1997). Hepatitis C virus diagnostics: technology, clinical applications and impacts. Trends Biotechnol. *15*, 71–76.
27. Hoffman, D., Hesselberth, J., and Ellington, A.D. (2001). Switching nucleic acids for antibodies. Nat. Biotechnol. *19*, 313–314.
28. Breaker, R.R. (2002). Engineered allosteric ribozymes as biosensor components. Curr. Opin. Biotechnol. *13*, 31–39.
29. Rajendran, M., and Ellington, A.D. (2002). Selecting nucleic acids for biosensor applications. Comb. Chem. High Throughput Screen. *5*, 263–270.
30. Sontheimer, E.J. (1994). Site-specific RNA crosslinking with 4-thiouridine. Mol. Biol. Rep. *20*, 35–44.
31. Ludwig, J., and Eckstein, F. (1989). Rapid and efficient synthesis of nucleoside 5′-o-(1-thiotriphosphates), 5′-triphosphates and 2′,3′-cyclophosphorothioates using 2-chloro-4h-1,3,2-benzodioxaphosphorin-4-one. J. Org. Chem. *54*, 631–635.